

Possibilities of Drag Reduction by the Use of Flexible Skin

DEZSO GYORGYFALVY*

The Boeing Company, Seattle, Wash.

A flexible aerodynamic surface is considered as a possible means of delaying transition and reducing skin-friction drag. The results of an extensive analytical study on boundary-layer instability and transition in incompressible Blasius-flow over a flexible surface are presented. A simple flexible skin model consisting of a taut membrane and an elastic base has been considered. The mechanical behavior of such a skin is controlled by the mass, the wave propagation velocity, the stiffness, and the damping. The analysis shows that with proper selection of the surface characteristics, the transition can be significantly delayed through reduced amplification rates, even though the critical Reynolds number for instability is only slightly increased. The extent of transition delay and the required surface properties are delineated. The theoretically possible drag reduction is most significant within the Reynolds number range of 3 to 50×10^6 . Hence, potential fields of application of flexible skins would be in sailplanes, helicopters, small and medium subsonic airplanes, hydrofoils, torpedoes, speed boats, and miniature submarines.

Nomenclature

- c_i = amplification factor, imaginary part of the complex wave velocity
 c_r = phase velocity, real part of the complex wave velocity
 C_{0m} = wave propagation velocity in the membrane, $(T/M)^{1/2}$
 d = damping coefficient, Eq. (21)
 D = damping constant, lb-sec/ft³
 K_M = mass parameter, Eq. (13)
 K_S = stiffness parameter, Eq. (15)
 K_D = damping parameter, Eq. (17)
 m = mass coefficient, Eq. (18)
 M = membrane mass per unit area, lb-sec²/ft³
 R_x = Reynolds number based on length, $U_\infty x/\nu$
 R_δ = Reynolds number based on boundary-layer thickness
 S = compression stiffness of base material, lb/ft³
 T = membrane tension, lb/ft
 U_∞ = freestream velocity, fps
 x = distance from leading edge along the plate, ft
 α = dimensionless wave number, $k\delta$
 β_r = disturbance frequency, αc_r
 δ = boundary-layer thickness, ft
 δ^* = boundary-layer displacement thickness, ft
 ν = kinematic viscosity of fluid, ft²/sec
 ρ = density of fluid, lb-sec²/ft³
 ω_0 = dimensionless cutoff frequency, $(S/M)^{1/2}\delta/U_\infty$
 ω^* = circular frequency of disturbance, sec⁻¹
 ω_r = dimensionless circular frequency, $\beta_r/R_\delta = \omega^*\nu/U_\infty^2$

Introduction

THE problem of reducing skin-friction drag, by the use of flexible surface coatings, has generated considerable interest in recent years. This new method of boundary-layer control is based upon the concept that a flexible surface, through proper coupling with the flow, can produce a favorable influence on the boundary layer and thus reduce skin-friction drag. The favorable influence may be either a delay of transition from laminar to turbulent flow, or possibly, a reduction of the shear stresses in a turbulent boundary layer. The present paper considers the potential for drag reduction due to transition delay.

Flexible skin for reducing skin friction was first proposed by Kramer¹ as a result of studies on the hydrodynamic per-

formance of dolphins. Experiments with flexible surface coatings having characteristics similar to the dolphin's skin showed impressive drag reductions in water. Inspired by Kramer's promising experimental results, Benjamin,² and Landahl³ conducted fundamental theoretical investigations concerning the effects of a flexible wall on hydrodynamic stability. It was found that a properly designed flexible surface would, indeed, have favorable effects on the boundary-layer stability, although the critical Reynolds number (at which instability first occurs) could be increased only by a relatively small amount. It was also found, however, that a flexible skin could introduce other types of instabilities which would be undesirable. Benjamin classified these as "class B" and "class C" instabilities to distinguish them from the basic Tollmein-Schlichting instability, termed "class A." (Class B represents a surface resonance type of instability and class C is a divergence type.) Furthermore, it was also recognized that damping in the surface is beneficial in preventing class B instability, but it is actually detrimental in stabilizing the Tollmein-Schlichting waves.

Following the previous theoretical studies, several experimental programs were undertaken with the aim of duplicating Kramer's results under different test environments. Most of these experiments, however, were unsuccessful or inconclusive. Perhaps the most important result emerging from these experiments has been the recognition that more specific theoretical foundations are required before one can expect consistent success in experimental work. The renewed interest in further developing the theory has produced several newer contributions, among which those of Kaplan,⁴ Landahl,⁵ and Benjamin⁶ are especially noteworthy.

The present study was motivated by recognizing that the principal effect of a flexible skin would be in reducing the amplification of the Tollmein-Schlichting waves rather than in postponing instability. Lower amplification rates then should lead to delayed transition, even though the neutral stability limits would not be significantly affected. Thus, the focus of interest in the present study was directed toward the effects of flexible skin on the amplification of the Tollmein-Schlichting waves and the transition delay attainable, whereas most previous studies have been concerned only with the neutral stability characteristics.

The principal objectives were to find to what extent the transition could be delayed by flexible skin, what properties the flexible skin should possess to delay transition effectively, what reductions in skin friction would be possible, and what the most promising fields of application would be.

Presented as Preprint 66-430 at the AIAA 4th Aerospace Sciences Meeting, Los Angeles, Calif., June 27-29, 1966; submitted June 22, 1966; revision received November 28, 1966. The author wishes to acknowledge the contributions of G. R. Hink, who developed the computer program used in this study. [3.01, 3.02]

* Aerodynamics Engineer, Aerodynamics Research Unit, Commercial Airplane Division. Member AIAA.

Fundamentals of the Theory

Neutral Stability Criterion

According to boundary-layer stability theory, transition occurs as a consequence of instability of small disturbances (Tollmein-Schlichting waves) developing in the laminar boundary layer because of surface roughness or turbulence in the main flow. After a certain degree of amplification, these waves burst into turbulent spots that spread downstream and change the character of the boundary layer from laminar to turbulent.

The conditions under which instability occurs are predicted by the stability theory. In its basic form, an incompressible, parallel, laminar boundary layer with a given mean velocity profile $U(y)$ is considered (Blasius flow), upon which small two-dimensional periodic disturbance velocities u and v are superimposed. Mathematically, the disturbance takes the form of a traveling wave that can be described by a stream function

$$\psi(x, y, t) = \phi(y)e^{ik(x-ct)} \quad (1)$$

where ϕ is the amplitude, k is the wave number, and c is the wave velocity. It is assumed that k is a real quantity, whereas c is complex, $c = c_r + ic_i$. The fundamental relation from which the stability of a disturbance can be determined is the Orr-Sommerfeld equation:

$$i\alpha R_\delta [(U-c)(\phi'' - \alpha^2\phi) - U''\phi] = \phi'''' - 2\alpha^2\phi'' + \alpha^4\phi \quad (2)$$

In Eq. (2), all variables are made dimensionless; those having a length scale are divided by δ , the velocities by U_∞ , the times by δ/U_∞ , and the pressures by ρU_∞^2 .

To solve Eq. (2), one must define the applicable boundary conditions. In the case of Blasius flow over a homogeneous flexible wall, the appropriate boundary conditions can be derived from the requirements that the disturbance velocities must vanish far from the wall and the motion of the fluid and the surface must be compatible at the interface. The second condition, in effect, means that the traveling wave admittances of the fluid and the surface must be equal at $y = 0$.

Solutions to the Orr-Sommerfeld equation are possible only for certain eigenvalue combinations of the parameters α , c , and R_δ . The behavior of a certain disturbance is determined by the imaginary part of the c eigenvalue. If $c_i < 0$, the disturbance is damped (i.e. the flow is stable) and if $c_i > 0$, the disturbance is amplified (i.e. the flow is unstable). The limiting case $c_i = 0$ corresponds to neutral stability.

The criterion for neutral stability in the case of a flexible wall was formulated by Landahl³ as

$$\Delta Y = Y_0 - Y = 0 \quad (3)$$

where Y_0 represents the fluid admittance for neutrally stable waves and Y denotes the mechanical admittance of the surface. The expression for Y_0 is given by

$$Y_0 = -\frac{i\alpha}{U_w'} \left[u + iv - \frac{\mathfrak{F}}{1 + \lambda(1 - \mathfrak{F})} \right] \quad (4)$$

where U_w' denotes the initial slope of the mean velocity profile; u and v are the perturbation velocity components that depend on α , c , and $U(y)$; λ is a factor depending on c and $U(y)$, and the quantity \mathfrak{F} is known as the modified Tietjens function $\mathfrak{F}(z) = \mathfrak{F}_r + i\mathfrak{F}_i$, where $z = c(\alpha R_\delta)^{1/3}/U_w'^{2/3}$. The calculation of these quantities is described in detail by Lin.⁷

For the Blasius profile, the factor λ is very small and may be neglected without causing a serious error. Thus, the neutral stability criterion, in simplified form, can be written as follows:

$$\Delta Y = -(i\alpha/U_w')[u + iv - \mathfrak{F}(z)] - Y = 0 \quad (5)$$

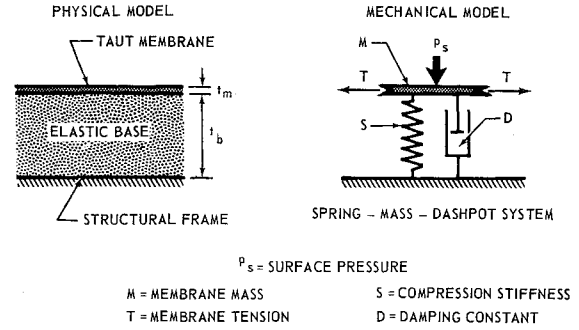


Fig. 1 The flexible skin model considered.

Mechanical Admittance of the Flexible Surface

The mechanical admittance of a flexible surface is a quantity describing the response of the surface to traveling pressure waves. By definition, the admittance is the reciprocal of the impedance, that is, the ratio of the displacement velocity amplitude to the pressure amplitude

$$Y = 1/Z = -\hat{v}_s/\hat{p}_s \quad (6)$$

In the present study, a simple flexible skin model is considered which consists of a thin, taut membrane supported by a foamlike elastic base. The mechanical behavior of the skin is determined by the mass, tension, stiffness and damping (Fig. 1). For the sake of analytical simplicity, the following assumptions are made: 1) the mass of the base material is negligible in comparison with the mass of the membrane; 2) the bending stiffness of the membrane is negligible; and 3) the damping, which is provided by the base material, is linear with the displacement velocity (viscous damping). Hence, the model skin can be treated as a continuous mass-spring-dashpot system for which the equation of motion can be written as

$$T \frac{\partial^2 \eta}{\partial x^2} - M \frac{\partial^2 \eta}{\partial t^2} - D \frac{\partial \eta}{\partial t} - S \eta = p_s \quad (7)$$

where p_s is the surface pressure and η is the surface displacement, both being represented by a traveling wave

$$\left. \begin{aligned} p_s &= \hat{p}_s e^{ik(x-ct)} \\ \eta &= \hat{\eta} e^{ik(x-ct)} \end{aligned} \right\} \quad (8)$$

From Eq. (7), one can derive the ratio of the pressure amplitude to the displacement amplitude:

$$\hat{p}_s/\hat{\eta} = Mk^2c^2 - Tk^2 - S + iDkc \quad (9)$$

and from this, the admittance is obtained by

$$Y = -\hat{v}_s/\hat{p}_s = ikc\hat{\eta}/\hat{p}_s \quad (10)$$

The expression for Y , however, must be given in a dimensionless form in order to make it compatible with Eq. (4). This is done in the same manner as described in connection with Eq. (2); namely, all lengths are divided by δ , velocities by U_∞ , etc. Letting $c_{0m} = (T/M)^{1/2}/U_\infty$ (the dimensionless propagation velocity of free surface waves in the membrane) and

$\omega_0 = (S/M)^{1/2}\delta/U_\infty$ (the cutoff frequency), one obtains

$$c_0 = (c_{0m}^2 + \omega_0^2/\alpha^2)^{1/2} \quad (11)$$

as the dimensionless wave propagation velocity for the composite skin. Furthermore, letting $m = M/\rho\delta$ (mass coefficient) and $d = D/\rho U_\infty$ (damping coefficient), the dimensionless surface admittance can be written as

$$Y = 1/d + im\alpha[(c_0^2/c) - c] \quad (12)$$

For the flexible skin model considered, the physical properties such as the mass per unit area, tension, stiffness, and

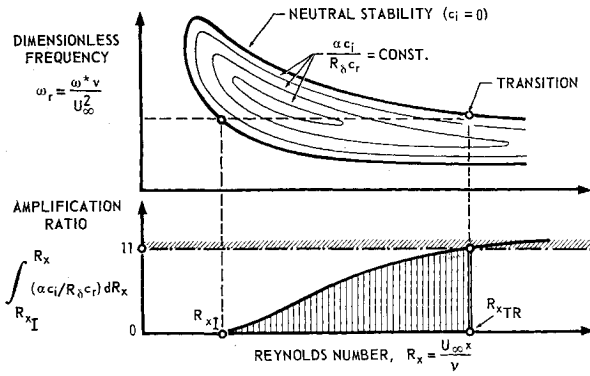


Fig. 2 Illustration of the transition calculation technique.

damping constant are uniform along the plate. This means that the dimensionless material coefficients in the admittance equation vary as δ , the boundary-layer thickness. For a general description of the surface characteristics, it is desirable to introduce dimensionless parameters that are independent of the boundary-layer thickness. For example

Mass Parameter

$$K_M = (R_1/\rho)M \quad (13)$$

Tension Parameter

$$K_T = T/\mu U_\infty \quad (14)$$

Stiffness Parameter

$$K_S = S/\mu U_\infty R_1^2 \quad (15)$$

Cutoff Frequency Parameter

$$K_\omega = (K_S/K_M)^{1/2} \quad (16)$$

Damping Parameter

$$K_D = 2\zeta = \Delta/\pi \quad (17)$$

where ζ is the damping factor, Δ is the logarithmic decrement, μ is the viscosity, and $R_1 = U_\infty/\nu$ is the unit Reynolds number. The material coefficients appearing in the admittance equation can be expressed with the above parameters as follows:

$$m = K_M/R_\delta \quad (18)$$

$$c_0 = [(K_T/K_M) + K_\omega^2 R_\delta^2/\alpha^2]^{1/2} \quad (19)$$

$$\omega_0 = K_\omega R_\delta \quad (20)$$

$$d = K_D K_M \alpha c_0 / R_\delta \quad (21)$$

Each coefficient is an explicit function of R_δ , which varies with the boundary-layer growth along the plate:

$$R_\delta \cong 6R_x^{1/2} \quad (22)$$

Amplification Rates

In addition to the eigenvalues corresponding to neutral stability, a series of eigenvalues can be found for the stability equation for which $c_i \neq 0$. Of these, the unstable eigenvalues ($c_i > 0$) are of further interest since they determine the amplification characteristics. The amplification of a traveling wave can be expressed by the ratio of any two consecutive amplitudes:

$$\frac{A_2}{A_1} = \exp \left(\int_{t_1}^{t_2} \beta_i dt \right) \quad (23)$$

where β_i is the temporal amplification rate, defined as the imaginary part of the complex frequency:

$$\beta = \beta_r + i\beta_i = \alpha(c_r + ic_i) \quad (24)$$

Several numerical techniques have been developed to calculate the amplification rates. Pretsch's⁸ and Shen's⁹ methods are best known of these. A simple, approximate technique was suggested by Landahl,³ and this has been used in the present study. Accordingly, the amplification factor c_i can be given by

$$c_i = -[\Delta Y/(\partial \Delta Y/\partial c)]_{c=c_r} \quad (25)$$

where c_r is the phase velocity at an eigenvalue. This simple relation, although justifiable only near the neutral stability boundary, gives reasonably good results throughout the entire unstable zone.

Transition Criterion

An unstable disturbance requires a certain degree of amplification before it can produce transition. The distance between the point of instability and point of transition can be predicted on the basis of an empirical correlation, found by A.M.O. Smith,¹⁰ between the theoretical amplification rates and the experimental point of transition. Using Pretsch's amplification rate charts, Smith calculated the rate of growth of the unstable Tollmein-Schlichting waves for a number of cases in which the actual point of transition had been known, and found that an amplification ratio of

$$\frac{A_{TR}}{A_I}(R_\delta) = \exp \left(\int_{t_I}^{t_{TR}} \beta_i dt \right) \cong \exp 9 \quad (26)$$

was characteristic at transition. From this correlation, Smith has formulated a transition criterion according to which transition occurs when the amplification ratio of the most critical frequency reaches the value of $\int \beta_i dt = 9$.

Pretsch's amplification rate charts give somewhat lower values for β_i than more recent calculation techniques. Accordingly, the critical value of $\int \beta_i dt$ at transition is greater than 9 when the amplification rates are calculated by some different technique than that of Pretsch. Using Eq. (25) for the calculation of c_i , the appropriate value of $\int \beta_i dt$ at transition was found to be approximately 11. For numerical evaluation of the transition point, it is necessary to express the temporal amplification rates in terms of spatial amplification rates, which can be done to the first approximation by substituting $dt = dx/c_r$.[†] Thus, the transition criterion

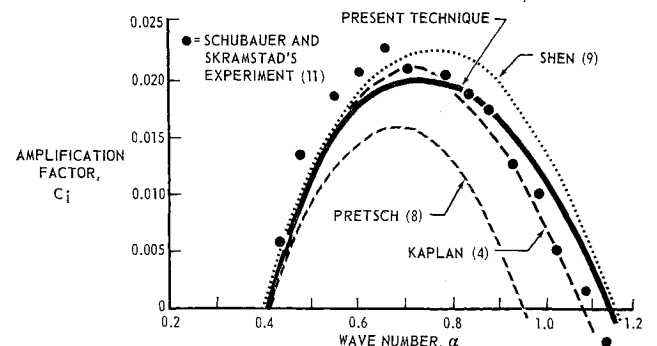


Fig. 3 Comparison of calculated and measured amplification factors (rigid surface, $R_\delta = 7700$, i.e., $R_\delta^* = 2200$).

[†] A more precise way of converting the temporal and spatial amplification rates is to use the group velocity, $c_g = \partial(\alpha c_r)/\partial \alpha$, instead of the phase velocity, c_r . The difference between c_g and c_r , however, is not too significant in ordinary cases.

applied in present analysis is as follows:

$$\int_{u_l}^{u_{TR}} \beta_i dt = \int_{R_{x_l}}^{R_{x_{TR}}} \left(\frac{\alpha c_i}{c_r R_\delta} \right) dR_x = 11 \quad (27)$$

It is known that in the later phase of the amplification process, the disturbances become three-dimensional and non-linear; thus, the existing conditions can no longer be validly described by the stability theory and the calculated amplification rates are rather fictitious. But in spite of this, Smith's correlation method has proved to be a useful way in predicting transition in the case of flows over rigid surface. We have postulated that this technique is also applicable in the case of flexible surface, and based our analysis, in great part, upon this assumption. It has been speculated,⁵ however, that the flexible skin might have a favorable influence not only on the development of the Tollmein-Schlichting waves, but also on the breakdown of these into three-dimensional waves in the later part of the amplification process, and if this is true, then the results of the present transition prediction technique might even be somewhat conservative.

Computation Technique

The previous concepts concerning neutral stability, amplification, and transition have been integrated into a computer program. This made it possible to carry out an extensive parametric study on the effects of a flexible skin on transition delay. The major steps of the computation procedure are as follows (Fig. 2).

1) The eigenvalues α and c corresponding to neutral stability ($c_i = 0$) are calculated for various selected x stations along the plate on the basis of Eq. (5). The eigenvalues define the neutral stability boundary that is presented in Fig. 2 in terms of $\omega_r = f(R_x)$, where ω_r is the dimensionless circular frequency ($\omega_r = \beta_r/R_\delta = \omega^* \nu/U_\infty^2$).

2) At each x station, the unstable zone between the upper and lower branches of the neutral stability curve is divided into equal intervals and at each of these points, the corresponding amplification factor c_i is calculated using Eq. (25). Thus, an $\alpha c_i/R_\delta c_r = f(\omega_r)$ curve can be defined for each x station selected. Then cross plots are made at various values of ω_r , and hence a set of $[\alpha c_i/R_\delta c_r = f(R_x)] \omega_r$ functions are generated.

3) The growth of the amplification ratio $\int (\alpha c_i/R_\delta c_r) dR_x$ is calculated along the plate for various values of ω_r and when the value of the integral reaches the critical value of 11, the transition criterion is satisfied. On this basis a curve is defined representing the predicted transition Reynolds number as a function of the disturbance frequency $R_{x_{TR}} = f(\omega_r)$. The lowest value of $R_{x_{TR}}$ is then the transition Reynolds number.

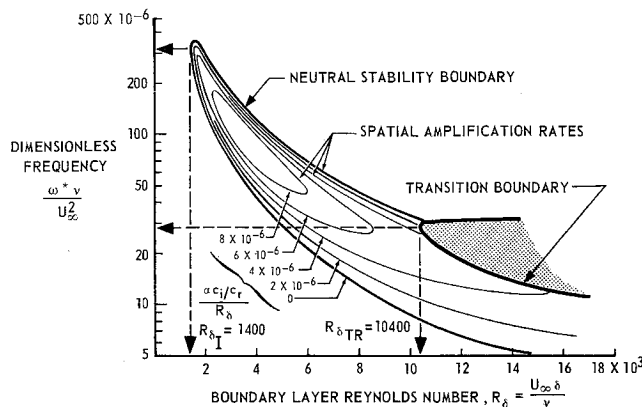


Fig. 4 The neutral stability boundary, spatial amplification rates, and the transition boundary as calculated by the present technique for a rigid flat plate.

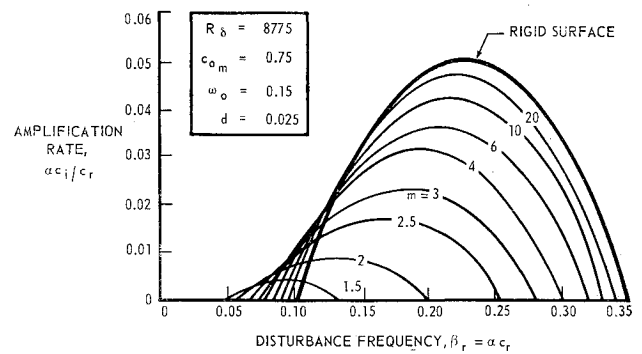


Fig. 5 Effect of mass coefficient on the amplification rates.

Review of Results in the Case of Rigid Surface

The accuracy of the present calculation technique can be verified by comparing its results with other theoretical and experimental data. This has been done for the case of rigid surface for which well-established data are available.

The amplification factors $c_i = f(\alpha)$ are compared in Fig. 3 for a given Reynolds number, showing the results of various calculation techniques together with Schubauer and Skramstad's¹¹ experimental data. Pretsch's results date from 1940 and are probably least accurate. Shen's data reflect the state-of-the-art of 1954, whereas Kaplan's data represent the more recent and refined calculations. The results of the present technique are in reasonably good agreement with the experimental and the newer theoretical data.

The complete set of information regarding instability and transition, as obtained by the present computer technique for a Blasius flow over rigid surface, is presented in Fig. 4. Included are 1) the neutral stability boundary $c_i = 0$, 2) the contour lines of equal amplification $\alpha c_i/c_r R_\delta = \text{const}$, and 3) the transition boundary $\int (\alpha c_i/c_r R_\delta) dR_x = 11$, plotted in terms of ω_r vs R_δ . The critical Reynolds number for instability is $R_{\delta I} = 1400$ ($R_{\delta I^*} = 400$), and for transition, it is $R_{\delta TR} = 10400$ ($R_{\delta TR^*} = 2980$). The corresponding length Reynolds numbers are $R_{x I} \cong 5.45 \times 10^4$ and $R_{x TR} \cong 3.0 \times 10^6$, respectively. The dimensionless critical frequency for instability is approximately $\omega_{r I} \cong 320 \times 10^{-6}$, and the frequency that first produces transition is $\omega_{r TR} \cong 28 \times 10^{-6}$. These results are in agreement with the generally accepted values. Unfortunately, similar comparisons cannot be made regarding flexible surfaces for lack of comparative data.

Effects of Flexible Surface Properties on the Amplification Rates

The speculation that the main effects of a flexible skin would be on the amplification rates rather than on the instability limits has proved to be correct. It will be demonstrated that the amplification rates can be significantly reduced if the properties of the surface are properly selected. The way in which the mass, the wave velocity, the stiffness, and the damping influence the amplification rates is illustrated in Figs. 5-8. The surface properties are specified by the coefficients m , c_0 , ω_0 , and d . In each case one property is variable while the other three are constant.

The effect of the mass coefficient $m = \rho_m t_m / \rho \delta$ is shown in Fig. 5. As m decreases, the amplification rates are reduced and the unstable zone is shifted toward lower frequencies. For $m > 10$, the reduction is relatively small, but for $m < 10$ it becomes more and more impressive: 15% at $m = 10$, 38% at $m = 4$, and 82% at $m = 2$. Obviously, the lowest possible mass coefficient is desired; the minimum attainable value of m is, however, limited by the density of practical membrane materials. This is especially critical in air

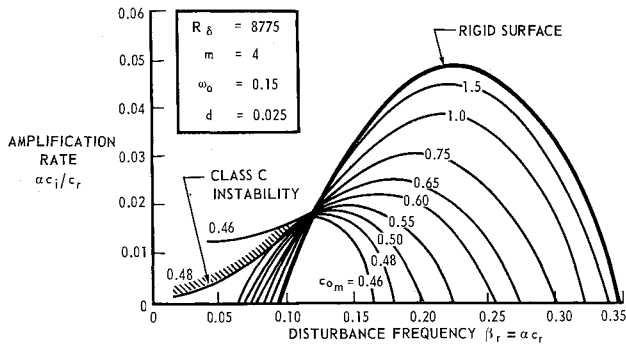


Fig. 6 Effect of membrane wave velocity on the amplification rates.

application when $\rho_m \gg \rho$; hence, $t_m \ll \delta$ would be required to provide a low value of m . Nevertheless, t_m cannot be reduced below certain limits for technological reasons. In water application, it is much easier to satisfy the requirements in regard to m since there are practical materials available which have comparable densities with that of water.

The effect of the membrane wave propagation velocity, $c_{0m} = (T/M)^{1/2}/U_\infty$ is shown in Fig. 6. The amplification rates decrease with decreasing c_{0m} , but significant reductions are possible only if $c_{0m} < 1.0$. On the other hand, c_{0m} cannot be lower than the phase velocity of the fastest unstable Tollmein-Schlichting waves. In the present case, this is approximately $c_{0m} = 0.48$. If c_{0m} is further decreased, divergence-type instability (class C) takes place at lower frequencies.

The effect of the cutoff frequency $\omega_0 = (S/M)^{1/2}\delta/U_\infty$ is shown in Fig. 7. The conditions are similar to those presented in Fig. 6; decreasing ω_0 reduces the amplification rates, but below a certain limit, which is between $\omega_0 = 0.09$ and 0.10 for the case shown, class C instability occurs.

The effect of the damping coefficient $d = D/\rho U_\infty$ is shown in Fig. 8. The amplification rates decrease with decreasing damping; thus again, as low a value of d as possible is desired. A certain amount of damping is required, however, to prevent a class B instability. It is interesting to note that high damping, for example, $d > 0.3$ in the case shown, may result in greater amplification rates than those associated with the rigid surface. It is not apparent from Fig. 8, but calculations for other cases have shown that the relative influence of the damping markedly depends on the accompanying values of m and c_{0m} . If these are relatively low, the effect of d on $\alpha c_i/c_r$ is very significant, whereas, if either m or c_{0m} is relatively high, the influence of d is small.

As to the optimum combination of surface characteristics, it is clear that the lowest possible values of m , c_{0m} , ω_0 , and d are desirable. The density and inherent damping of suitable

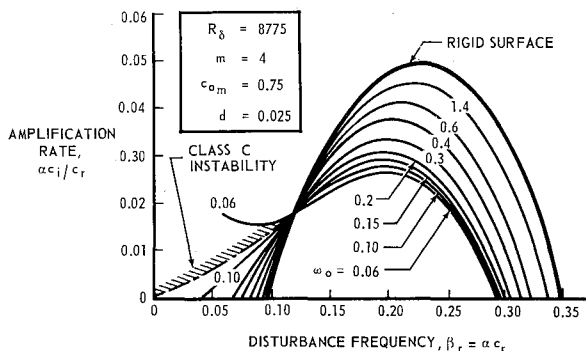


Fig. 7 Effect of cutoff frequency on the amplification rates.

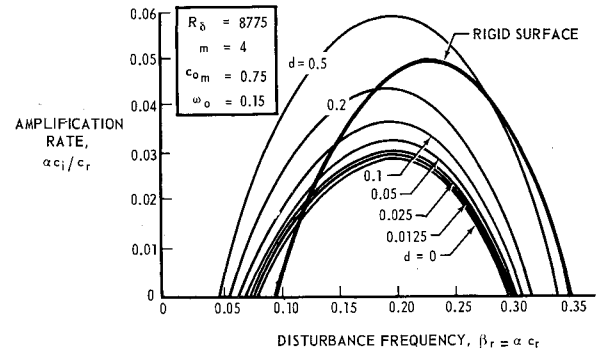


Fig. 8 Effect of damping on the amplification rates.

materials, as well as the occurrence of secondary instabilities (class B and C), however, put limitations on the minimum attainable values of these coefficients. These limits depend partly on the specific combination of the variables and also on the associated value of R_δ . The best results, that is, maximum reductions in the amplification rates, could be expected from such a flexible surface in which the minimum values of the coefficients m , c_{0m} , ω_0 , and d are maintained from point to point along the plate. Because of the growth of the boundary layer, this would require continuously changing surface properties, that is, a so-called "tailored" skin. Although a certain degree of tailoring is possible, for example, by varying the thickness of the membrane or the base layer, etc., it would be very difficult to design a surface with constant m , c_{0m} , ω_0 , and d . For the simplified flexible skin model considered in this study, it is assumed that the physical properties, namely, the mass per unit area, surface wave velocity, compression stiffness, and damping factor, are constant. Consequently, the coefficients m , c_{0m} , ω_0 , and d must vary along the plate according to the variation of δ . The most important effect of this is that the mass coefficient, being proportional to $1/\delta$, is relatively high in the beginning, and reduces to the desired lower values only at some distance downstream. This implies that the instability point and the initial amplification rates will not be affected noticeably and that the beneficial effects of the flexible skin can be utilized only further downstream. One must strive, of course, to extend the region of effectiveness as far forward as possible by keeping the mass per unit area at the lowest possible level.

Effects of Surface Flexibility on the Transition Point

The effect of surface flexibility on the transition point will be first demonstrated by a numerical example. The calculated instability and transition boundaries are shown in Fig. 9 for a given flexible surface and for a rigid surface. It is seen that the onset of instability remains unaffected and only a seemingly minor shift occurs in the neutral stability limits;

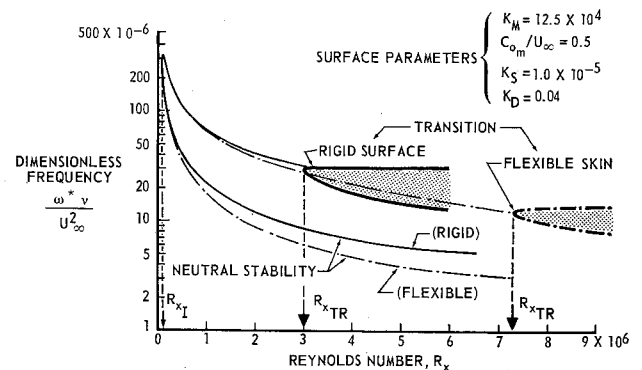


Fig. 9 Effect of a given flexible skin on neutral stability and transition.

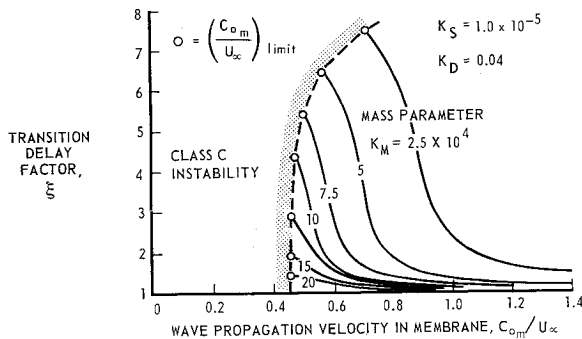


Fig. 10 The transition delay factor as affected by the mass and wave propagation velocity.

but the transition point is significantly delayed and the frequency band critical for transition is narrowed. Lower amplification rates associated with the flexible skin make possible the transition delay. The critical Reynolds number corresponding to transition is increased from $R_{x_{TR}} = 3 \times 10^6$ (rigid surface) to $R_{x_{TR}} = 7.2 \times 10^6$. The ratio of the critical Reynolds numbers, or, in other words, the ratio of the laminar lengths, is indicative of the efficiency of the flexible skin. We will call this ratio the transition delay factor:

$$\xi = \frac{R_{x_{TR}(\text{flexible surface})}}{R_{x_{TR}(\text{rigid surface})}} = \frac{x_{TR(\text{flexible surface})}}{x_{TR(\text{rigid surface})}} \quad (28)$$

In the present example we get $\xi = 2.4$, but considerably higher values are attainable with more favorable combinations of the surface parameters.

An extensive parametric study was carried out to determine the best combinations of surface properties and the extent of possible transition delay. Figure 10 demonstrates the variation of the transition delay factor as a function of the membrane wave velocity for various values of the mass parameter. With decreasing wave velocity, ξ increases until the limit of divergence (class C instability) is reached. This occurs at approximately $C_{0m}/U_{\infty} = 0.475$ for the higher values of the mass parameter ($K_M > 12 \times 10^4$), and at gradually increasing C_{0m}/U_{∞} 's in the case of lower K_M 's. The greatest transition delay is obtainable right at the divergence limit, and the corresponding membrane wave velocity is denoted as $(C_{0m}/U_{\infty})_{\text{limit}}$. On the other hand, there is no appreciable transition delay above a certain value of C_{0m}/U_{∞} , which is somewhere between 0.6 and 1.2, depending on the mass parameter. The latitude of favorable operation thus can be defined as the difference between $(C_{0m}/U_{\infty})_{\text{limit}}$ and the value of C_{0m}/U_{∞} at which the transition delay factor begins to grow.

The decisive influence of the mass parameter is clearly seen in Fig. 10. Low mass results not only in greater transition

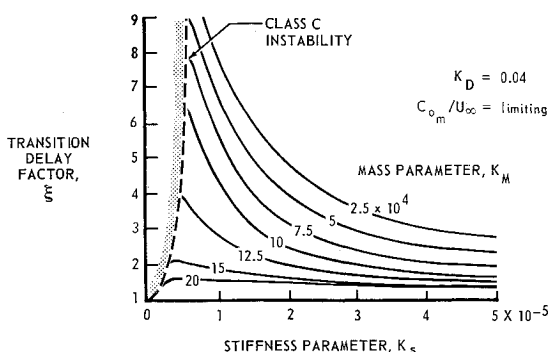


Fig. 11 The transition delay factor as affected by the mass and stiffness.

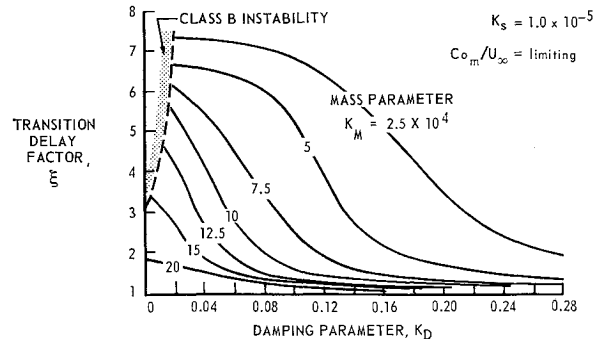


Fig. 12 The transition delay factor as affected by mass and damping.

delay but also in a greater latitude of favorable operation velocities. The difficulties associated with finding membrane materials of sufficiently low mass density but still of adequate strength constitute the major problem for the aeronautical application. In this case, lower values of the mass parameter than $K_M = 10 \times 10^4$ probably would not be attainable.

The effects of the stiffness and damping on the transition delay factor are shown in Figs. 11 and 12, respectively, for various values of the mass parameter and the limiting value of the membrane wave propagation velocity. Decreasing stiffness or decreasing damping results in a greater transition delay, but the occurrence of class C instability at low values of K_S or of class B instability at low values of K_D limits the minimum allowable values of these parameters. In the light of the limitations affecting the selection of surface parameters, it is estimated that transition delay factors up to $\xi = 4$ in air and $\xi = 10$ in water could be ultimately attained.

Drag Reduction Potentials

From an engineering point of view, the most important question is to find out how much drag reduction would be possible by the use of flexible skin. The effect of delayed transition on the smooth flat-plate skin friction is demonstrated in Fig. 13, where C_F is shown as a function of the Reynolds number, R_L (based on the plate length), for various values of the transition delay factor. The parameter $\xi = 1$ represents the case of a rigid surface for which the transition occurs at $R_{x_{TR}} = 3 \times 10^6$. Below this Reynolds number ($R_L < R_{x_{TR}}$), the skin friction is purely laminar; above it, the $C_F = f(R_L)$ curve is determined on the basis of a partly laminar, partly turbulent boundary layer. With delayed transition, this curve is shifted toward higher Reynolds numbers. Thus $\Delta C_F = C_{F_{\text{rigid}}} - C_{F_{\text{flex}}}$ represents the drag reduction attainable at a given R_L by delaying the transition. This potential drag reduction is shown in Fig. 14 as a percentage of the rigid flat plate skin-friction coefficient for

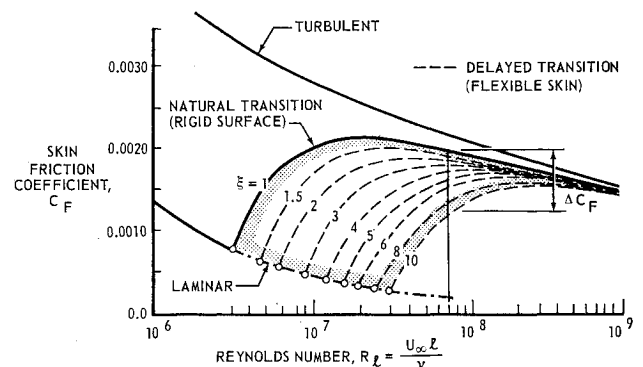


Fig. 13 Effect of delayed transition on the flat plate skin-friction coefficient.

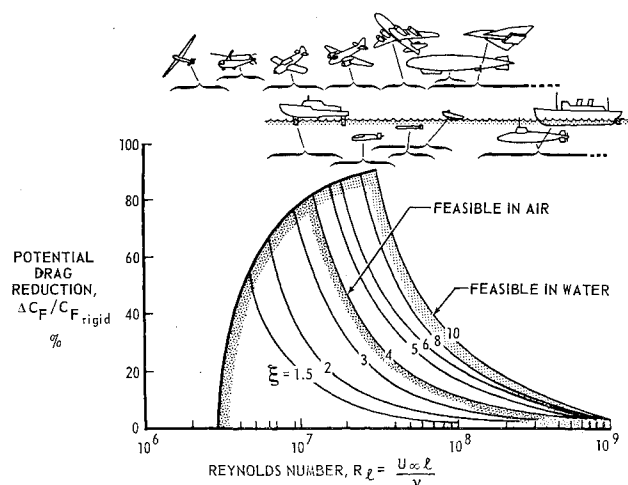


Fig. 14 Potential drag reduction due to transition delay and operation Reynolds number ranges of various airborne and waterborne vehicles.

various values of ξ . The theoretically possible drag reduction is indeed very impressive; it exceeds 50% of $C_{F_{rigid}}$ within the Reynolds number range of 4.2 to 19×10^6 in the case of $\xi = 4$, and 4.2 to 56×10^6 in the case of $\xi = 10$, with peak values of $\Delta C_F / C_{F_{rigid}} = 80$ and 90% , respectively. At high Reynolds numbers, however, the opportunities are quite limited, especially in air application.

In order to illustrate the potential fields of application for flexible skin, the operational Reynolds number ranges of various airborne and waterborne vehicles are also included in Fig. 14. It is seen that the greatest drag reduction potentials would be available in the Reynolds number domain of helicopter rotor blades, small and medium size subsonic airplanes, as well as hydrofoils, midsize submarines, torpedoes, and small speed boats. Large and fast vehicles such as modern jet transports, supersonic airplanes, blimps, ships, submarines, etc., seem to fall out of the favorable Reynolds number range.

It is to be noted that in the case of practical surfaces with nonzero pressure gradients and surface roughness, the transition Reynolds number is usually lower than $R_x = 3 \times 10^6$; hence, the curves of Fig. 14 would be shifted to the left. Thus, sailplanes also could be considered as a possible field of application, but on the other hand, the drag reduction potentials at higher Reynolds numbers would be accordingly lower.

Conclusions

Summarizing the results of the present study on the possibilities of transition delay by flexible skin, the following conclusions can be made.

1) The main effect of a flexible skin is on the amplification of the Tollmein-Schlichting waves rather than on the instability limits. With proper selection of the flexible surface characteristics, the amplification of the Tollmein-Schlichting waves can be significantly reduced and accordingly the transition can be delayed.

2) The flexible skin is characterized by four physical properties: mass per unit area, surface wave velocity, stiffness, and damping. Each of these must be within certain tolerances to make the skin effective. The most stringent requirement is low mass. The surface wave propagation velocity must be slightly higher than the phase velocity of the Tollmein-Schlichting waves, that is, somewhere between 50 to 80% of the freestream velocity. Higher values make the skin ineffective; lower values lead to increased instability.

The stiffness and damping should be as low as possible but certain values are required to prevent divergence or resonance-type instabilities.

3) The possibilities of transition delay are greater in water application than in air application because of the lower values of relative mass (ρ_{skin}/ρ_{fluid}) attainable in water. It will be very difficult indeed to find practical materials of sufficiently low density, especially in aeronautical application. Preliminary estimates suggest that transition delays of up to 4 times in air and up to 10 times in water could ultimately be achieved. The associated reduction in skin-friction drag is very significant (up to 80% in air and 90% in water) but it is attainable only within a rather narrow Reynolds number range. The most promising fields of application for flexible skin are in those vehicles that operate at Reynolds numbers of about 3 to 50×10^6 .

4) A logical follow-up of the present study would be an attempt to verify these theoretical results by a carefully conducted experiment. The theoretical work should also be continued by investigating other types of flexible skin models and the possibilities of "tailored" skin. Extension of the calculation technique to flows with pressure gradient and to compressible flow would also be desirable.

5) The possibilities of skin friction reduction by flexible skin are by no means exhausted in this study. Even greater opportunities seem to open up through development of an "active" flexible skin, that is, one in which surface waves, providing a favorable coupling with the flow, are artificially generated. Another opportunity of great significance is the development of flexible skins which would reduce turbulent skin friction. Realization of these opportunities requires continued and extensive research efforts along both theoretical and experimental lines.

References

- Kramer, M. O., "Boundary layer stabilization by distributed damping," *J. Am. Soc. Naval Engrs.* **72**, 25-33 (1960); also **74**, 341-348 (1962).
- Benjamin, T. B., "Effects of a flexible boundary on hydrodynamic stability," *J. Fluid Mech.* **9**, 513-532 (1960).
- Landahl, M. T., "On the stability of a laminar incompressible boundary layer over a flexible surface," *J. Fluid Mech.* **13**, 609-632 (1962).
- Kaplan, R. E., "The stability of laminar incompressible boundary layers in the presence of compliant boundaries," ScD Thesis, Massachusetts Institute of Technology, Aeroelastic and Structures Research Lab., TR 116-1 (1964).
- Landahl, M. T. and Kaplan, R. E., "The effect of compliant walls on boundary layer stability and transition," *Proceedings of the AGARD Fluid Dynamics Panel Conference on Boundary Layer Technology, Naples, Italy, May 1965* (Technical Editing and Reproduction Ltd., London, England, 1965), pp. 363-394.
- Benjamin, T. B., "Fluid flow with flexible boundaries," *Proceedings of the 11th International Congress of Applied Mechanics* (Springer-Verlag, Berlin, 1966), pp. 109-128.
- Lin, C. C., "On the stability of two-dimensional parallel flows," Pts. I, II and III, *Quart. Appl. Math.* **3**, 117-142, 218-234, 277-301 (1945).
- Pretsch, J., "The excitation of unstable perturbations in a laminar friction layer," NACA TM 1343 (1952).
- Shen, S. F., "Calculated amplified oscillations in the plane Poiseuille and Blasius flows," *J. Aeronaut. Sci.* **21**, 63-64 (1954).
- Smith, M. O. and Gamberoni, N., "Transition, pressure gradient, and stability theory," Douglas Co. Rept. ES 26388 (1956).
- Schubauer, G. B. and Skramstad, H. K., "Laminar boundary layer oscillations and transition on a flat plate," NACA TR 909 (1948).